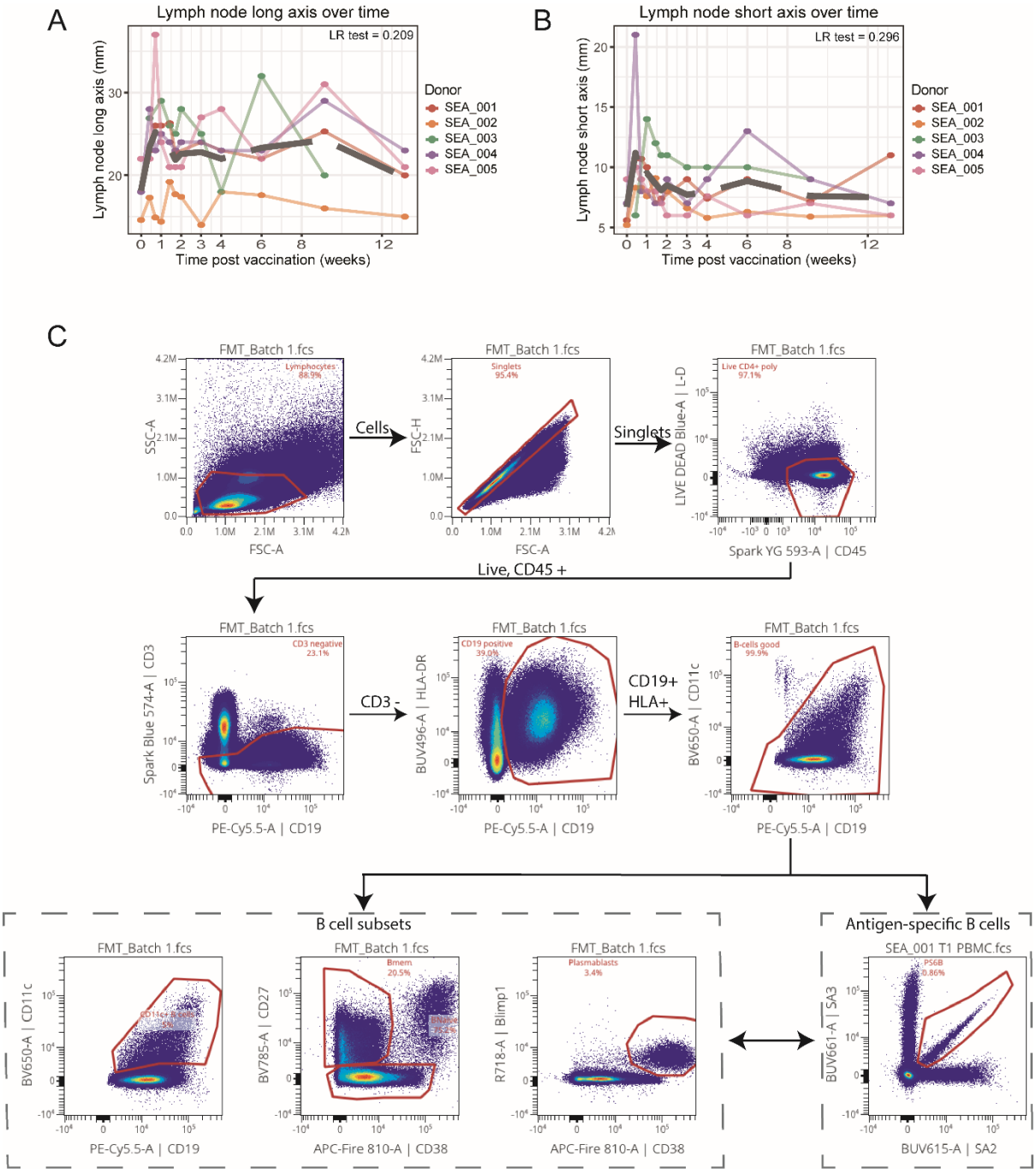
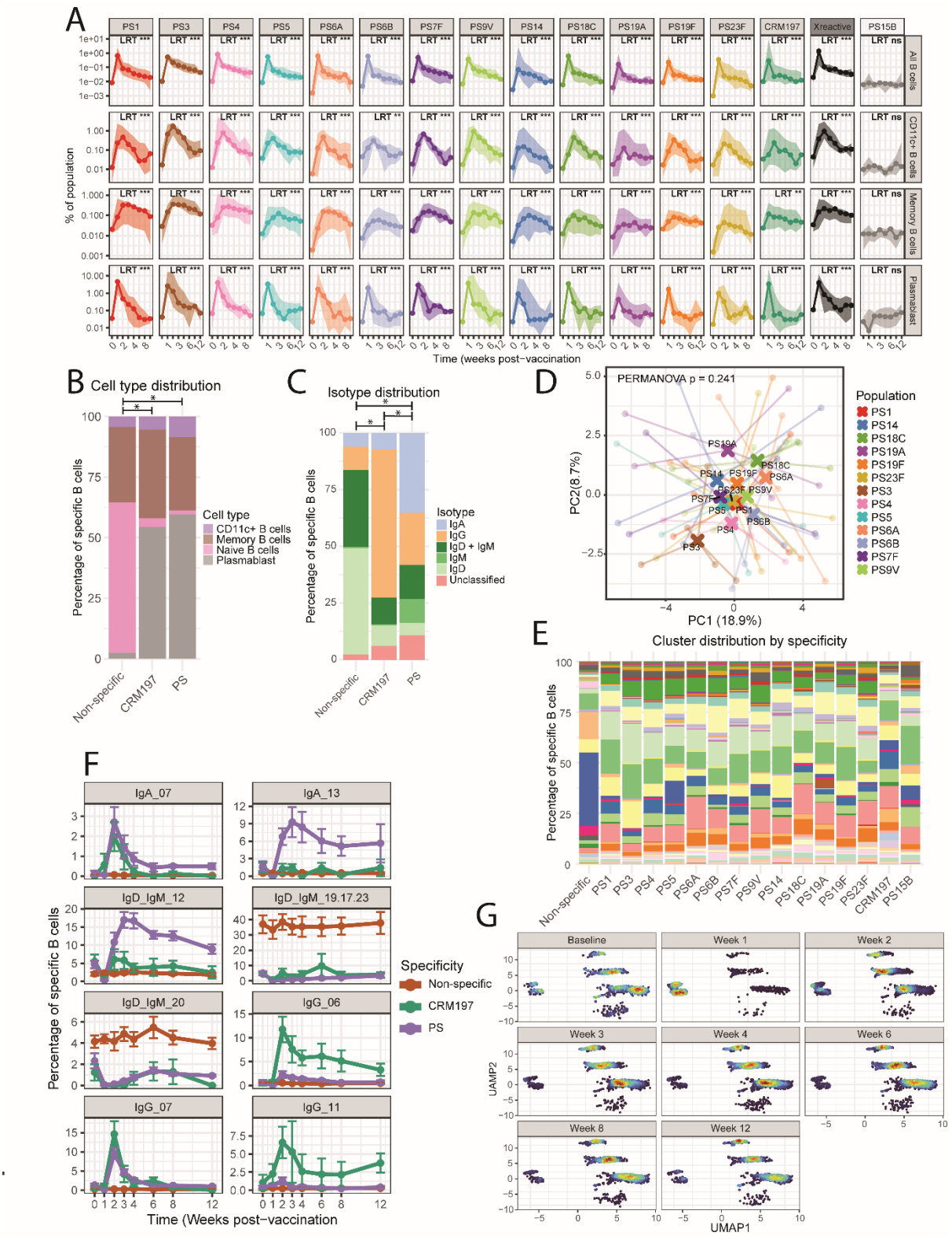
Supplemental Table 1. Antibodies used for flow cytometry staining

Marker	Fluorochrome	Clone	Isotype	Vendor	Catalog #	Dilution	Stain mix
CD185	BUV395	RF8B2	Rat	BD	740266	25	CXCR pre-stain
CD184	BUV805	12G5	Mouse IgG2a	BD	742043	25	CXCR pre-stain
CD25	BV605	BC96	Mouse IgG1	BD	567571	50	Surface
CD71	BUV737	LO1.1	Mouse IgG2a	BD	748311	50	Surface
CD197	BV480	3D12	Rat IgG2a	BD	566099	50	Surface
CD127	BB700	hIL-7R-M21	Mouse IgG1	BD	566398	50	Surface
CD279	RB744	EH12.1	Mouse IgG1	BD	570478	100	Surface
CD3	Spark Blue 574	UCHT1	Mouse IgG1	Biolegend	300488	100	Surface
CD27	BV785	0323	Mouse IgG1	Biolegend	302832	100	Surface
CD45RA	BV570	HI100	Mouse IgG2b	Biolegend	304132	300	Surface
CD38	APC-Fire810	HIT2	Mouse IgG1	Biolegend	303550	300	Surface
CD278	BV750	C398.4A	Hamster IgG	Biolegend	313558	300	Surface
CD95	PE-Vio770	DX2	Mouse IgG1	Miltenyi	130-123-887	300	Surface
CD11c	BV650	Bu15	Mouse IgG1	Biolegend	337238	400	Surface
IgD	Pacific Blue	IA6-2	Mouse IgG2a	Biolegend	348224	200	Surface
HLA-DR	BUV496	G46-6	Mouse IgG2a	BD	569674	600	Surface
CD45	Spark YG593	HI30	Mouse IgG1	Biolegend	304084	600	Surface
IgG	BV510	G18-145	Mouse IgG1	BD	563247	300 / 800	Surface / ICS
CD45RB	PE	MEM55	Mouse IgG2b	Biolegend	310204	600	Surface
CD86	PE-Cy5	IT2.2	Mouse IgG2b	Biolegend	305408	800	Surface
CD8	Spark Blue 550	SK1	Mouse IgG1	Biolegend	344760	1600	Surface
CD19	PE-Cy5.5	SJ25C1	Mouse IgG1	eBioscience	35-0198-42	800	Surface
CD43	BV421	1G10	Mouse IgG1	BD	562916	1600	Surface
CD4	Pacific Blue	RPA-T4	Mouse IgG1	Biolegend	300521	800	Surface
IgM	Spark Blue 550	MHM-88	Mouse IgG1	Biolegend	314556	800	Surface
IgA	APC-Vio770	IS11-8E10	Mouse IgG1	Miltenyi	130-113-473	800 / 19600	Surface / ICS

FoxP3	Spark NIR685	206D	Mouse IgG1	Biolegend	320130	50	ICS
Bcl-6	PE-Dazzle 594	7D1	Rat IgG2a	Biolegend	358510	200	ICS
Blimp-1	R718	6D3	Rat IgG2a	BD	567764	200	ICS
Ki-67	RB780	B56	Mouse IgG1	BD	568761	15000	ICS
Streptavidin	BUV563			BD	612935		Multimer / ICS
Streptavidin	BV711			Biolegend	405207		Multimer / ICS
Streptavidin	BB515			BD	564453		Multimer / ICS
Streptavidin	APC			Biolegend	405207		Multimer / ICS
Streptavidin	BUV615			BD	613013		Multimer / ICS
Streptavidin	BUV661			BD	612979		Multimer / ICS



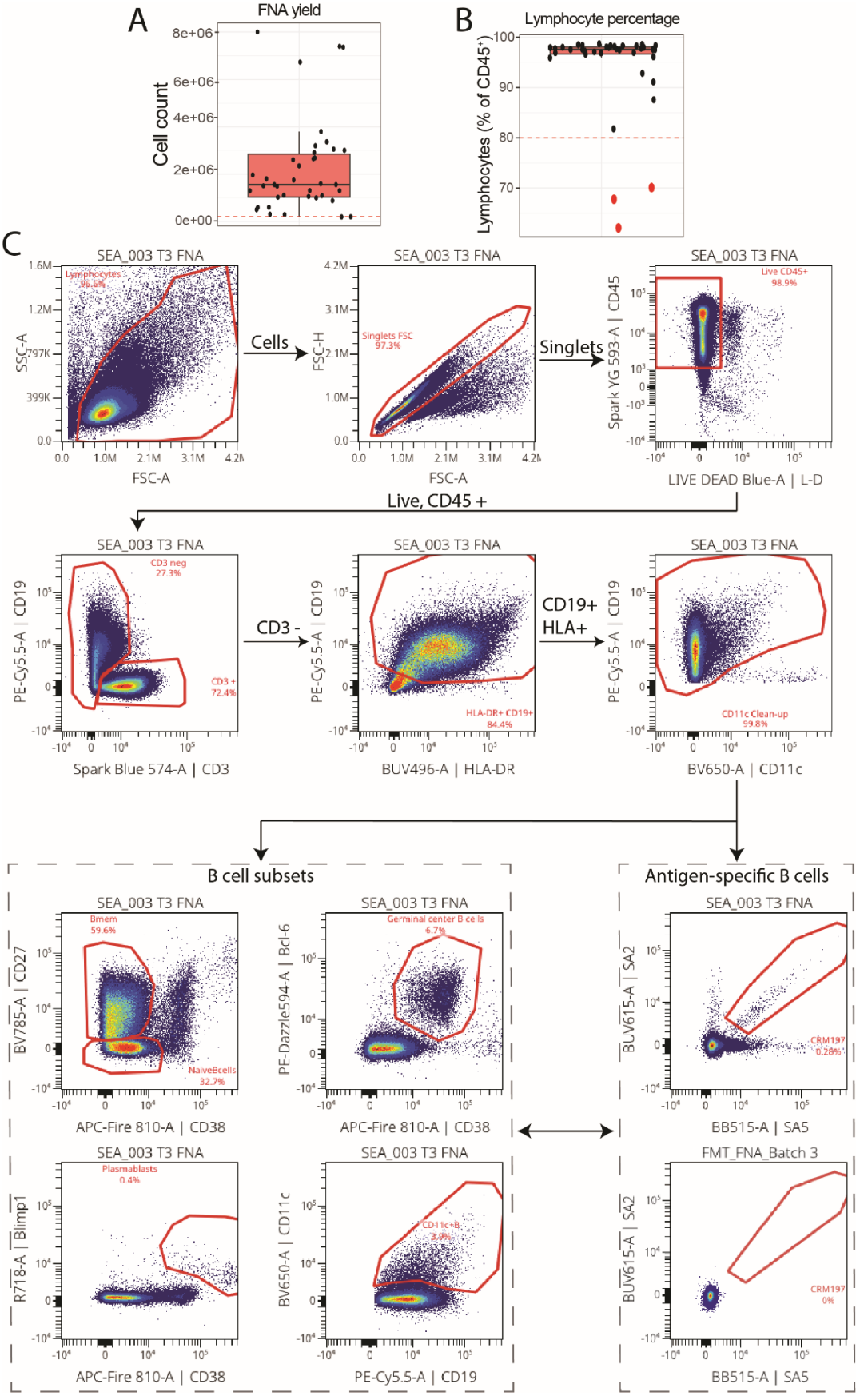
Supplemental Figure 1. PBMC gating strategy. Lymph node long axis **(A)** and short axis **(B)** as measured by ultrasound. Colored lines represent individual donor trajectory; grey bolded line represents the median. **(C)** Gating strategy to define B cell subsets and antigen-specific B cells in peripheral blood. B cells were defined based on CD19 and HLA-DR expression in CD3-, CD45+ live lymphocytes. Contaminant myeloid cells were removed based on low expression of CD19 and high expression of CD11c. Plasmablasts were defined based on their expression of CD38 and Blimp1, whereas CD27 and CD38 were used to define memory and naïve B cells. Antigen-specific B cells were defined using a barcoding scheme; example plot is shown for one specificity including the fluorescence minus multimers control below.


A
PS1
PS3
PS4
PS5
PS6A
PS6B
PS7F
PS9V
PS14
PS18C
PS19A
PS19F
PS23F
CRM197
Xreactive
PS15B
All B cells
CD11c+ B cells
Memory B cells
Plasmablast
% of population
Time (weeks post−vaccination)
B Cell type distribution
Percentage of specific B cells
Cell type
CD11c+ B cells
Memory B cells
Naive B cells
Plasmablast
Non-specific
CRM197
PS
C Isotype distribution
Isotype
IgA
IgG
IgD + IgM
IgM
IgD
Unclassified
D
PERMANOVA p = 0.241
PC1 (18.9%)
PC2(8.7%)
Population
E
Cluster distribution by specificity
F
IgA_07
IgA_13
IgD_IgM_12
IgD_IgM_19.17.23
IgD_IgM_20
IgG_06
IgG_07
IgG_11
Specificity
Non-specific
CRM197
PS
Time (Weeks post−vaccination)
G
Baseline
Week 1
Week 2
Week 3
Week 4
Week 6
Week 8
Week 12
UMAP1
UMAP2

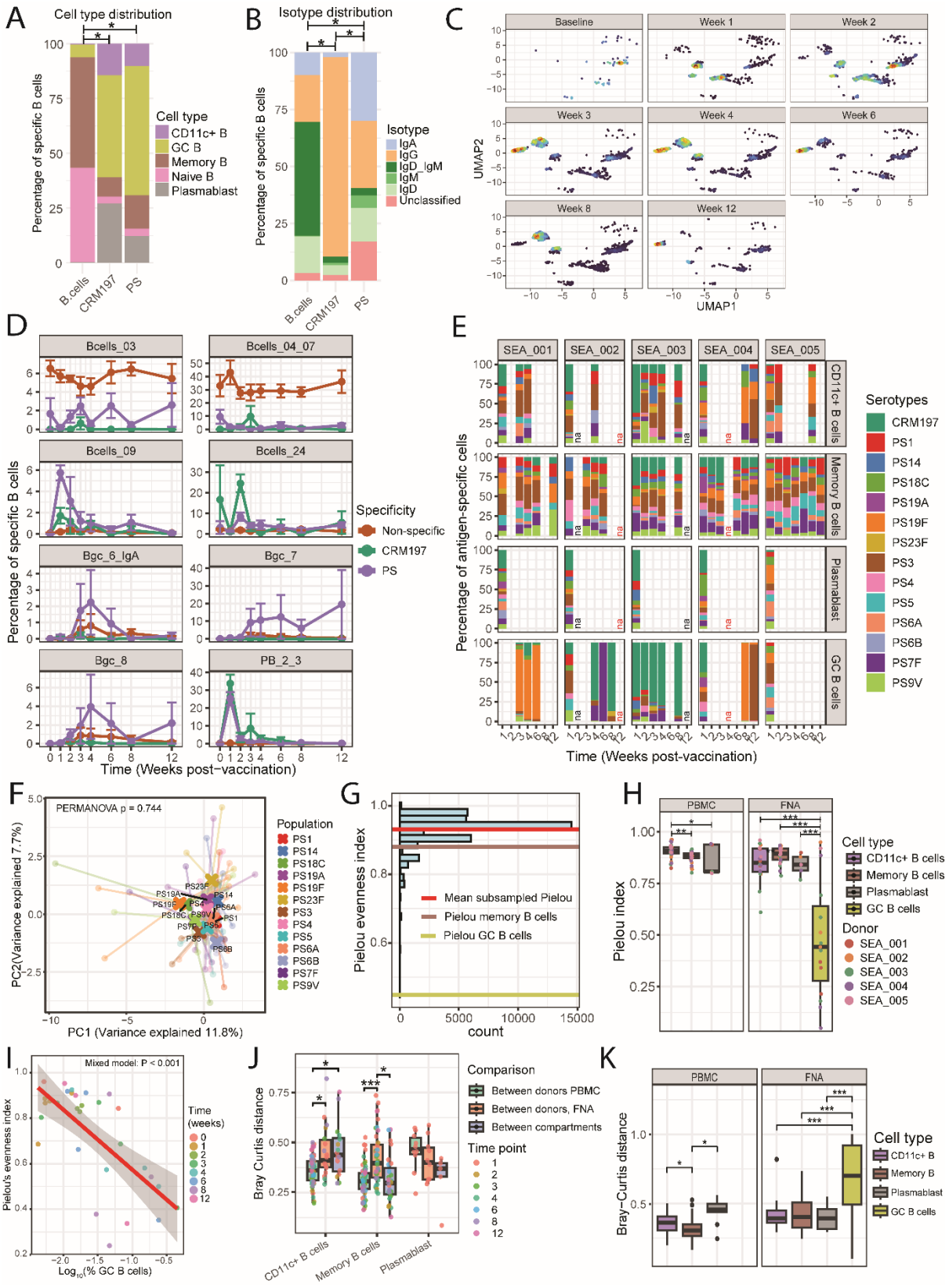
Supplemental Figure 2. B cell phenotype in PBMCs. (A) Kinetics of antigen-specific B cells for each specificity across major B cell subsets. Bolded line represents the sample median, shaded area represents the range. **(B)** Overall B cell phenotype was compared between specificities, aggregating across all serotypes for polysaccharides-specific B cells. Data shown represent mean frequencies across all samples. **(C)** Overall isotype expression is compared between specificities. Data shown represent mean frequencies across all samples. **(D)** PCA was performed to compare cluster distribution between polysaccharide-specific cells targeting different serotypes. Faint dots represent individual donors, while bolded crosses represent the centroids for each serotype. **(E)** Overall cluster distribution across cells of different specificities. Data shown represents mean cluster distribution across all donors and timepoints. **(F)** Kinetics plots of select clusters shown in Figure 2F. Data shown represent median cluster frequency within each specificity, with error bars showing SE. **(G)** UMAP projection showing dynamic changes of antigen-specific (Both CRM197 and PS- specific) B cell phenotype over time. Equal numbers of PS-specific and CRM197-specific cells at each timepoint were used as input for UMAP.

Expansion of antigen-specific B cells was assessed using a GLMM-based LR test. Comparisons between groups were done using PERMANOVA. Correction for multiple testing was done using the Benjamini Hochberg method.

* $p < 0.05$, ** $p < 0.01$, *** $p < 0.001$


A
FNA yield
Cell count
8e+06
6e+06
4e+06
2e+06
0e+00
B
Lymphocyte percentage
Lymphocytes (% of CD45+)
100
90
80
70
C
SEA_003 T3 FNA
Lymphocytes
86.6%
SSC-A
FSC-A
Cells
Singlets FSC
97.3%
FSC-H
Singlets
Live CD45+
98.9%
Spark YG 593-A | CD45
LIVE DEAD Blue-A | L-D
Live, CD45 +
CD3 neg
27.3%
CD3 +
72.4%
PE-Cy5.5-A | CD19
Spark Blue 574-A | CD3
CD3 -
HLA-DR+ CD19+
84.4%
BUV496-A | HLA-DR
CD19+
HLA+
CD11c Clean-up
99.8%
BV650-A | CD11c
B cell subsets
Antigen-specific B cells
Bmem
59.6%
NaiveBcells
32.7%
BV785-A | CD27
APC-Fire 810-A | CD38
Germinal center B cells
6.7%
PE-Dazzle594-A | Bcl-6
CRM197
0.28%
BUV615-A | SA2
BB515-A | SA5
Plasmablasts
0.4%
R718-A | Blimp1
CD11c+B
3.9%
BV650-A | CD11c
PE-Cy5.5-A | CD19
FMT_FNA_Batch 3
CRM197
0%

Supplemental Figure 3. Gating strategy in lymph node FNA samples. (A) Yield of FNA samples as determined by manual counting. **(B)** Purity of lymph node samples was determined by fresh acquisition of FNA samples and determining the percentage of lymphocytes among CD45+ events. Samples were excluded when lymphocyte percentage was < 80%. **(C)** Gating strategy to define B cell subsets and antigen-specific B cells in lymph node FNA. B cells were defined based on CD19 and HLA-DR expression in CD3-, CD45+ live lymphocytes. Contaminant myeloid cells were removed based on low expression of CD19 and high expression of CD11c. Plasmablasts were defined based on their expression of CD38 and Blimp1 and GC B cells based on CD38 and Bcl-6 expression. Memory B cells and naïve B cells were defined based on CD27 and CD38. Antigen-specific B cells were defined using a barcoding scheme; example is shown for one specificity including the fluorescence minus multimers below.

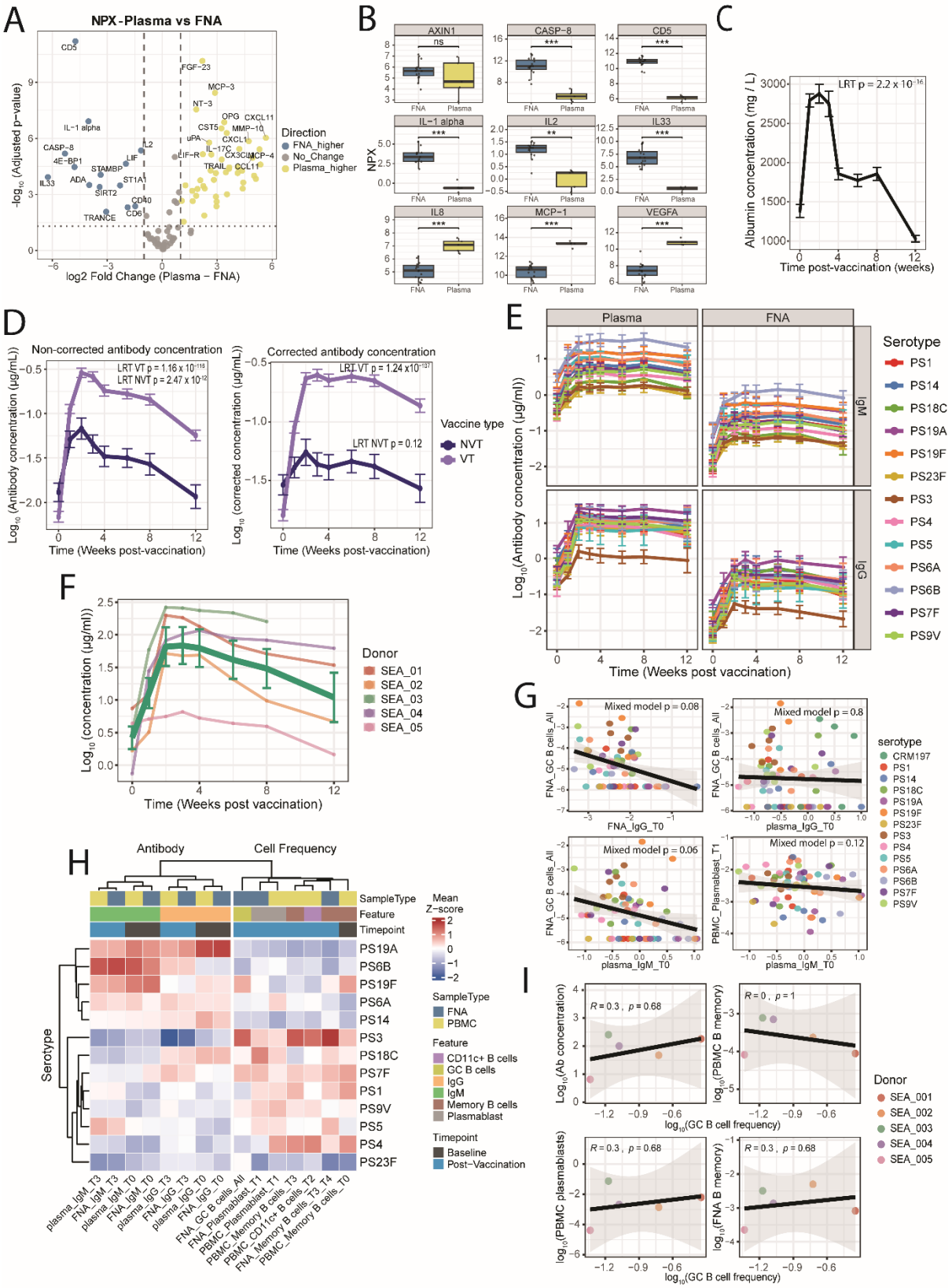


Supplemental Figure 4. Antigen-specific B cell phenotype in lymph node FNA samples. (A) Major B cell subsets were defined, and overall B cell phenotype was compared between different specificities. Data shown represent mean frequencies across all samples. **(B)** Overall isotype expression was compared between specificities. Data shown represent mean frequencies across all samples. **(C)** UMAP projection of CRM197 and PS-specific B cells for each time point, demonstrating phenotypic changes

of these cells over time. **(D)** Kinetics of select clusters in figure 4F, comparing kinetics of different specificities. Data shown represent mean +- SE. **(E)** Normalized serotype distribution of lymph node B cells across different B cell subsets for each donor and timepoint. Missing samples are indicated in black, while samples failing QC are indicated in red. Subsets having less than 10 serotype-specific cells were excluded from the analysis. **(F)** PCA was performed to compare cluster distribution between polysaccharide-specific cells targeting different serotypes. Faint dots represent individual donors, while bolded crosses represent the centroids for each serotype. **(G)** Pielou evenness index was calculated across 1000 iterations of randomly subsampling 10 antigen-specific peripheral blood memory B cells from each sample. The distribution of the calculated Pielou evenness index is shown. The red line represents the mean Pielou index obtained from random subsampling, the brown line represents the true mean Pielou index of peripheral memory B cells and the yellow line represents the true mean Pielou index of GC B cells. **(H)** Pielou index was compared between cell types within peripheral blood and lymph nodes. Samples with <10 serotype-specific cells were excluded from the analysis. **(I)** Pielou evenness was associated with lymph node GC B cell frequencies. Red line represents the regression line, shaded area indicates the confidence interval. **(J)** Bray-curtis distance between serotype distribution was calculated. Inter-donor variation was assessed using the within subset distance between donors, whereas inter-compartment variation was quantified using the within donor distance between compartments. **(K)** Between donor Bray Curtis distance for serotype distribution was quantified and compared between B cell subsets.

Comparisons between groups were performed using GLMM, followed by post-hoc emmeans based comparisons. Differences in serotype-specific B cell phenotype were tested using PERMANOVA. Correction for multiple testing was done using the BH method.

* $p < 0.05$, ** $p < 0.01$, *** $p < 0.001$



Supplemental Figure 5. Soluble factors can be measured in FNA supernatant. (A) Volcano plot comparing NPX values of soluble factors between plasma and FNA supernatant. Colored dots represent factors that differ significantly between matrices. Top 15 hits on either side were annotated. **(B)** NPX values as measured by Olink, highlighting some of the top hits identified in (A). **(C)** Albumin

concentration was measured in FNA supernatant as a measure for total protein content. Data shown represent median albumin concentration over time +- SE. **(D)** Antibody concentration for vaccine-type and non-vaccine-type pneumococcal serotypes were measured in lymph node FNA supernatant. Left panel shows uncorrected antibody concentrations, while right panel shows antibody concentrations after correction for albumin content. Data shown represent mean concentration across all specificities and donors +- SE. **(E)** IgM and IgG concentration against all vaccine serotypes as measured in plasma and FNA supernatant. Lines and points indicate mean concentration; error bars signify standard error. **(F)** CRM197 IgG concentration in plasma. Faint, coloured lines represent individual donor trajectories, while bold dark green line represents the sample mean. Error bars indicate SE. **(G)** Kendall correlation was performed (Figure 5E) and selected scatter plots are highlighted here. **(H)** Relative antibody concentrations and antigen-specific B cell frequencies were compared between serotypes. Z scores were calculated within each sample and averaged between samples. **(I)** Spearman correlation analysis was performed between GC B cell frequency and the CRM97 response, including CR197 IgG (top left), CRM197 memory B cells in peripheral blood (top right), CRM197-specific plasmablasts in peripheral blood (bottom left) and CRM197-specific memory B cells in the lymph node (bottom right). Black lines represent the regression line, while shaded areas indicate the confidence interval.

Global time effects were tested using LR test based on GLMMs. Differences between plasma and FNA NPX were assessed using a GLMM, followed by posthoc emmeans-based comparisons. Kendall correlation significance was assessed using GLMMs, using baseline values as the predictor. Correlation analysis between the CRM response and the GC B cell response was performed using Spearman correlation. Correction for multiple testing was done using the Benjamini Hochberg method.

* $p < 0.05$, ** $p < 0.01$, *** $p< 0.00$